



HAL
open science

Benchmarking a lattice-Boltzmann solver for reactive flows: Is the method worth the effort for combustion?

Pierre Boivin, M. Tayyab, S. Zhao

► **To cite this version:**

Pierre Boivin, M. Tayyab, S. Zhao. Benchmarking a lattice-Boltzmann solver for reactive flows: Is the method worth the effort for combustion?. *Physics of Fluids*, 2021, 33 (7), pp.071703. 10.1063/5.0057352 . hal-03276189

HAL Id: hal-03276189

<https://hal.science/hal-03276189v1>

Submitted on 1 Jul 2021

HAL is a multi-disciplinary open access archive for the deposit and dissemination of scientific research documents, whether they are published or not. The documents may come from teaching and research institutions in France or abroad, or from public or private research centers.

L'archive ouverte pluridisciplinaire **HAL**, est destinée au dépôt et à la diffusion de documents scientifiques de niveau recherche, publiés ou non, émanant des établissements d'enseignement et de recherche français ou étrangers, des laboratoires publics ou privés.

Benchmarking a Lattice-Boltzmann solver for reactive flows: Is the method worth the effort for combustion?

P. Boivin,^{1, a)} M. Tassyab,¹ and S. Zhao¹

Aix Marseille Univ, CNRS, Centrale Marseille, M2P2, 13451, Marseille, France

(Dated: 10 June 2021)

This letter reports a validation of a Lattice-Boltzmann approach following the Taylor-Green Vortex benchmark presented at the 19th International Congress on Numerical Combustion, and recently reported by Abdelsamie et al. in *Computers & Fluids*, 223, p. 104935 (2021). The Lattice-Boltzmann approach, despite having a time-step bound by an acoustic Courant–Friedrichs–Lewy condition, results being faster than the low-Mach solvers which participated to the benchmark. Such feat is made possible by the fully explicit nature of the method, and indicates very high potential for practical applications.

Lattice-Boltzmann methods^{1,2} (LBM), have led to stark cost reductions for the simulation of unsteady low-Mach athermal flows. The fields of aerodynamics and aeroacoustics were particularly impacted by the introduction of LBM, with costs reduced by close to an order of magnitude^{3–9}.

Owing to this success, numerous models were proposed to extend the LB capabilities from mono-component isothermal to multi-component reactive flows^{10–20}. With the same objective, we recently proposed a hybrid LB framework able to tackle compressible flows^{21,22}, and successfully applied it to multiple canonical combustion problems²³, combustion instabilities²⁴ and simulation of turbulent bluff-body stabilised flame²⁵.

As for unsteady athermal flows, one of the main motivations of applying LBM to reactive flows is the hope of slashing costs of unsteady reactive flows simulations, which remain nowadays very expensive for complex geometries, despite the constant progress in high-performance computing.

Nonetheless, research efforts to adapt LBM to reactive flows remained more limited than those aiming at simulating multiphase flow²⁶ or compressible flows^{21,27}. The authors attribute this to the widespread idea that LBM cannot lead to significant gain for reactive flows, because (i) multiple distributions are a priori required to solve multi-component flows and (ii) the cost of transport and kinetics in any reactive flow solver represents a significant share of the global cost. Nonetheless, recent studies⁹ indicate that most CPU cost associated to classical methods is lost in communication and memory transfer between processors, indicating that the answer may be more complex.

This letter’s objective is to present a validation of the approach on a well-documented DNS benchmark for reactive flows²⁸, and provide answers on this question: *Is the method worth the effort for combustion ?*

The numerical simulations are carried out with the PROLB software using a pressure-based compressible

Lattice Boltzmann (LB) model²² coupled with a Finite Differences (FD) solver^{23–25}. Its inherent massively-parallel solver includes an octree mesher which efficiently handles both complex geometries²⁹ and multi-resolution refinement layers³⁰.

Details on the algorithm may be found in our previous studies^{22–25} and are not repeated here. Besides the change of paradigm, from classical Navier-Stokes to Lattice-Boltzmann, the method is equivalent^{22,31} to solving the following macroscopic equations

$$\frac{\partial \rho}{\partial t} + \frac{\partial \rho u_\beta}{\partial x_\beta} = 0, \quad (1)$$

$$\frac{\partial \rho u_\alpha}{\partial t} + \frac{\partial \rho u_\alpha u_\beta + p \delta_{\alpha\beta} - \mathcal{T}_{\alpha\beta}}{\partial x_\beta} = 0, \quad (2)$$

where ρ is the volume mass, u_α is the local velocity vector and p is the pressure, obeying the multi-component perfect gas law. $\mathcal{T}_{\alpha\beta}$ is the stress tensor,

$$\mathcal{T}_{\alpha\beta} = \rho \nu \left(\frac{\partial u_\alpha}{\partial x_\beta} + \frac{\partial u_\beta}{\partial x_\alpha} - \delta_{\alpha\beta} \frac{2}{3} \frac{\partial u_\gamma}{\partial x_\gamma} \right). \quad (3)$$

The FD solver coupled with the above is responsible for solving species and energy conservation. For each species k ,

$$\rho \frac{\partial Y_k}{\partial t} + \rho u_\alpha \frac{\partial Y_k}{\partial x_\alpha} = \frac{\partial}{\partial x_\alpha} (-\rho Y_k V_{k,\alpha}) + \dot{\omega}_k, \quad (4)$$

where Y_k is the mass fraction of species k , $\dot{\omega}_k$ is its net chemical production rate, and $V_{k,\alpha}$ the diffusion velocity³². To match the approach followed by the Low-Mach codes participating in the study²⁸, the energy conservation is solved in its enthalpy form³²

$$h = \sum_{k=1}^N h_k Y_k, \quad h_k = \int_{T_0}^T C_{p,k}(T) dT + \Delta h_{f,k}^0, \quad (5)$$

where T and h are linked through NASA polynomials leading to the following enthalpy equation

$$\rho \frac{\partial h}{\partial t} + \rho u_\alpha \frac{\partial h}{\partial x_\alpha} = \frac{\partial p}{\partial t} - \frac{\partial q_\alpha}{\partial x_\alpha} + \mathcal{T}_{\alpha\beta} \frac{\partial u_\alpha}{\partial x_\beta}, \quad (6)$$

^{a)}Electronic mail: pierre.boivin@univ-amu.fr

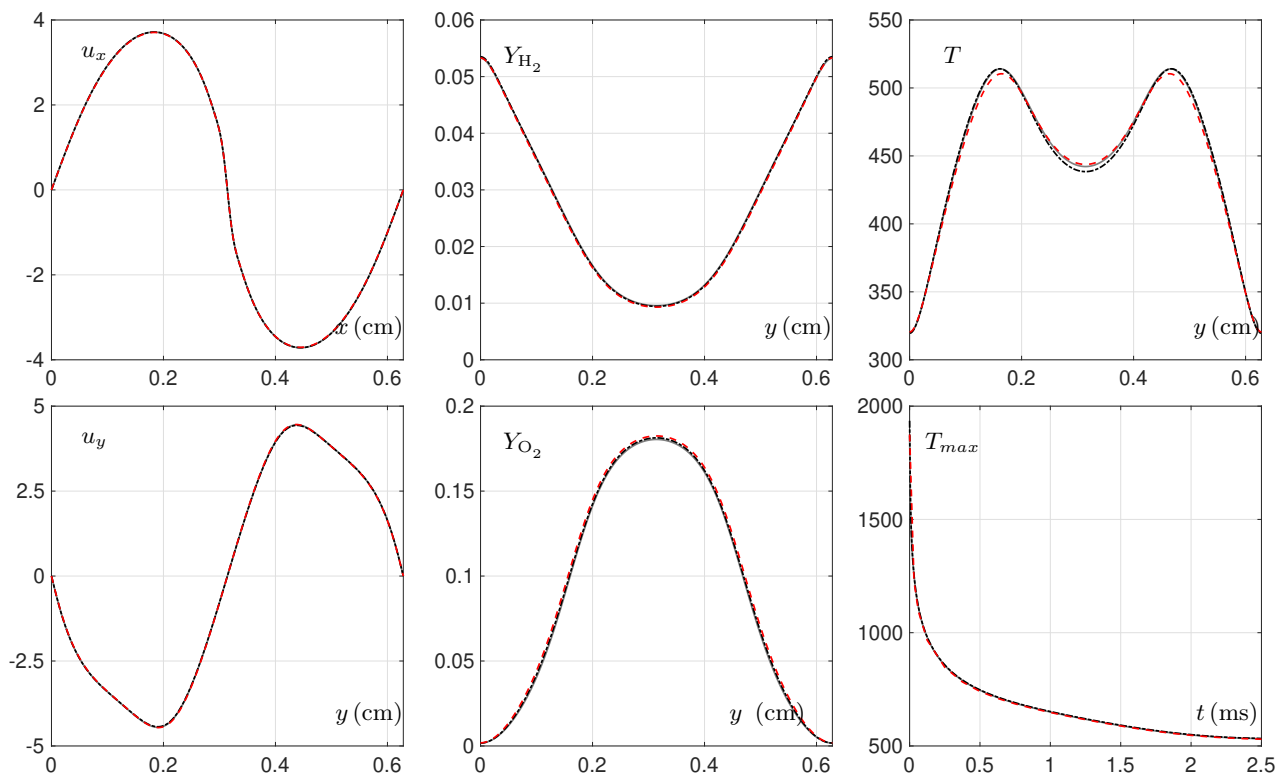


FIG. 1. Results of the non-reactive case at 0.5ms. Profiles obtained on the middle axis identified in the bottom right of each plot: u_x (m s^{-1}), u_y (m s^{-1}), Y_{H_2} , Y_{O_2} and Temperature (K). The last plot corresponds to the maximum temperature (K) in the domain over time. Yales (solid line), NEK (dashed-dotted line), ProLB (red dashed line).

where the heat flux q_α reads

$$q_\alpha = -\lambda \frac{\partial T}{\partial x_\alpha} + \rho \sum_{k=1}^N h_k Y_k V_{k,\alpha}, \quad (7)$$

with λ the thermal conductivity. Diffusion velocities are defined as in²³, using constant Schmidt number for each species, and a correction velocity to ensure mass conservation³². As reported in our previous studies^{22,23}, the method is second order accurate in both space and time, as classical LBM solvers². The order of accuracy of the method is nonetheless subject to caution, as LBM and classical solvers are known to exhibit different dissipation properties³³.

To validate our approach, let us follow the benchmark proposed recently by Abdelsamie et al.²⁸. The benchmark consists of four test cases:

- Step 1: 2D cold flow, single component,
- Step 2: 3D cold flow, single component,
- Step 3: 3D non-reacting multi-species flow,
- Step 4: 3D reacting mixture.

Results obtained for single-component steps 1 & 2 are provided in Supplementary material, and the remainder of this letter focuses on multi-species tests 3 & 4. Steps 3 & 4 are Taylor Green Vortex configurations with the following characteristics:

- 9 components are considered, corresponding to the species of a detailed hydrogen-air combustion mechanism^{34,35}.
- Transport properties correspond to constant Lewis numbers (but distinct for each species).
- In Step 4 (hereafter referred as *hot case*), a 12 step skeletal hydrogen-air mechanism^{35,36} is considered. Step 3 (*cold case*) is identical to step 4, with the source term turned off (e.g. $\dot{\omega}_k = 0$)

For a full description of the test cases, the reader is reported to²⁸.

Simulations were carried out using Aix-Marseille University mesocentre's facilities, consisting of 32 cpu per Dell PowerEdge C6420 node, powered by Intel Xeon Gold 6142 (Sky Lake) processors 2.6GHz. In the following, we compare the results obtained with ProLB on a 256^3 grid, with the results reported by Abdelsamie et al.²⁸ with two low-Mach codes on the same grid:

Yales 2: a massively parallel multi-physics platform developed at CORIA (see Yales2's webpage), fourth

order in space and time.

NEK5000: an open-source spectral reactive flow solver (see NEK5000’s webpage) for which a reactive flow plugin was developed at ETH Zurich.

Note that results from a third code – DINO – are also reported in the study²⁸. They were not included in the Figures here for the sake of readability, but are in excellent agreement with the two other codes²⁸.

Our simulations were performed with a constant time-step of $\Delta t = 1.5625 \times 10^{-8}$ s, corresponding to a maximum acoustic CFL number 0.6 defined as

$$\text{CFL} = \frac{\max(|u| + |c|)\Delta t}{\Delta x}. \quad (8)$$

Comparisons for the non-reacting multi-species flow (Step 3) are provided in Fig. 1, for u_x , u_y , Y_{H_2} , Y_{O_2} and temperature center line profiles. The last plot of Fig. 1 shows the maximum temperature evolution on the center line. Results are seen to be fully in line with the results reported by Abdelsamie *et al.*²⁸, showing that ProLB reproduces accurately the mixing in a complex multi-species non-isothermal flow.

Next, the 12 step skeletal hydrogen-air chemistry³⁷ is activated, to let the mixture ignite in the midst of the Talor-Green Vortex. Figure 2 presents profiles of:

- Velocity (u_x, u_y),
- Hydrogen mass fraction Y_{H_2} ,
- Heat release, indicating the flame structure,
- temperature,

on the axes retained by the authors of the benchmark²⁸. Also reported is the domain maximum temperature evolution over time. Velocity profiles show excellent agreement. A similar agreement is obtained for temperature profile and history. Minor discrepancies are observed on mass fraction and heat release plots, but are seen to be within the code to code deviation for this resolution level.

Figure 3 reproduces the top right temperature plot from Fig. 2, as obtained for 3 different resolutions: 128^3 , 256^3 , 384^3 . The maximum temperatures obtained for these resolutions are respectively 1770K, 1757K, 1756K (1758K in the reference study²⁸), corresponding to relative errors of 7.1×10^{-3} , -6.2×10^{-4} and -1.2×10^{-3} , respectively. Errors of the same order are reported in the reference study.

Computing costs are indicated in Tab. I, reporting:

- N_p , the number of grid points,
- N_{cores} , the number of cores used,
- N_{iter} , the number of iterations to reach T_{sim} ,
- T_{sim} , the total simulated physical time,

- $\overline{\Delta t}$, the simulation time-step,
- TCPU, the total number of cpu hours,
- $\text{RCT} = \frac{\text{TCPU}}{N_{\text{iter}} \times N_p}$, the reduced computational time²⁸,
- $\text{RTTS} = \frac{\text{TCPU}}{T_{\text{sim}} \times N_p}$, the reduced time to solution²⁸.

By comparison, the reduced computational time (RCT) is reduced by an order of magnitude compared to the fastest low-Mach code for both cold and hot cases. This result was expected, as the present method is fully explicit, and thus requires a much smaller time-step. Because of that small time-step, the LB approach does not come close to low-Mach solvers reduced time to solution (RTTS), for the cold flow.

That gap is filled, nonetheless, when considering hot flow. Because of their implicit treatment of kinetic and diffusion terms, Yales2 and NEK5000 require a drastic increase in RCT (resp. by a factor 4.5 and 6.5), whereas DINO and ProLB are relatively unaffected by the inclusion of source terms. Overall, ProLB ends up producing results 37% faster than the most efficient low-Mach code of the benchmark.

A major advantage of the present approach is that it is fully compressible. Via introduction of an adequate numerical scheme for the energy equation²⁷, it is possible to replace the enthalpy equation (6) by the total energy equation at no additional cost. In other words, the computational cost reported here should be compared with compressible codes, for which no published results are available up to date. Such approaches typically cost five times more than their low-Mach counterparts. Note, nonetheless, that results considering a total energy equation may slightly differ, and should be compared with compressible codes.

A second advantage is that, in LBM, the sound speed may easily be modified in low-Mach configurations, by artificially reducing the sound speed by a given factor. This can be done straightforwardly for the cold case, as long as the Fourier stability condition remains satisfied, while further scaling would require an implicit treatment of diffusion terms. For the hot case, a similar treatment can be applied, even though the short chemical time-scales would quickly require implicit treatment, significantly increasing the RCT.

We showed that our hybrid Lattice-Boltzmann method^{22–25,27,38} is competitive for the simulation of multi-species reacting flows. Following the benchmark by Abdelsamie *et al.*²⁸, we showed that LBM can provide compressible results for less than the cost of classical low-Mach solvers. In conclusion, our hybrid LBM approach^{22–25,27,38} is a promising and competitive method for combustion applications.

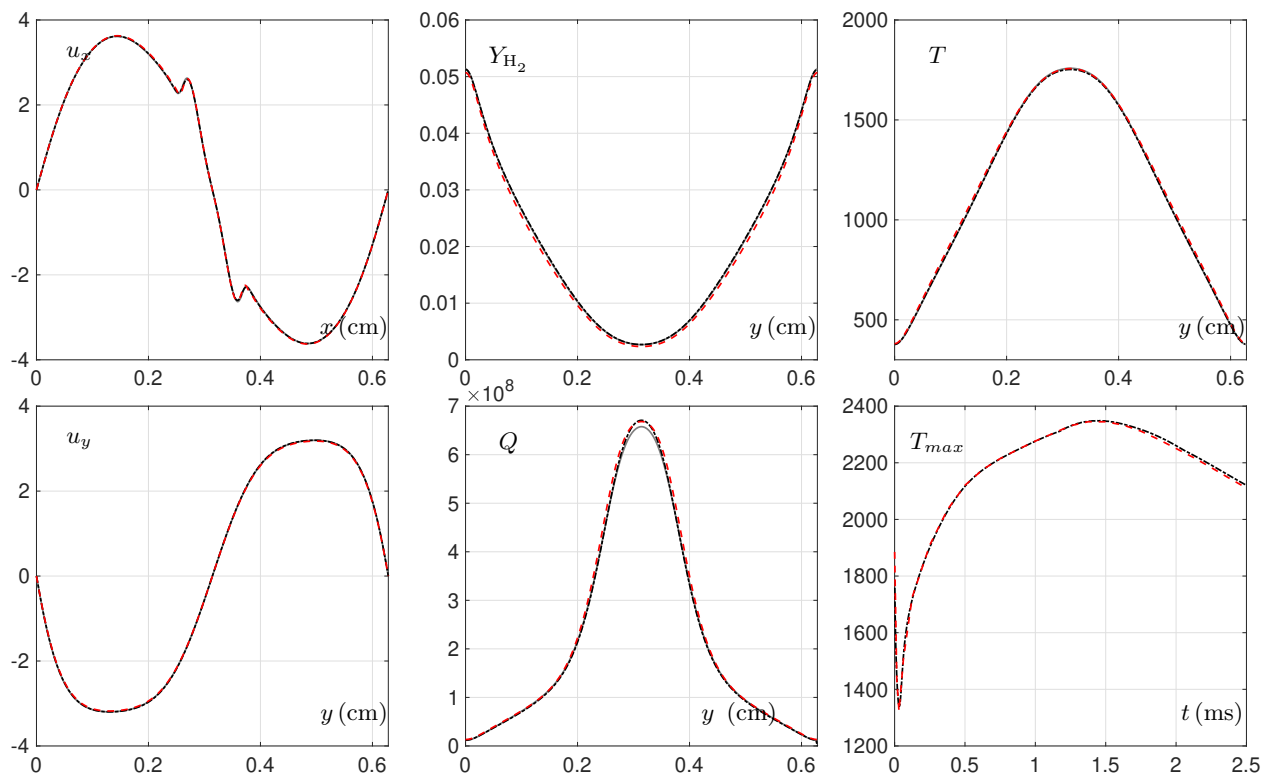


FIG. 2. Results of the reactive case at 0.5ms. Profiles obtained on the middle axis identified in the bottom right of each plot: u_x (m s^{-1}), u_y (m s^{-1}), Y_{H_2} , Q (W m^{-3}) and Temperature (K). The last plot corresponds to the maximum temperature (K) in the domain over time. Yales (solid line), NEK (dashed-dotted line), ProLB (red dashed line).

Solver	N_p	N_{cores}	N_{iter}	T_{sim}	$\overline{\Delta t}$	TCPU	RCT	RTTS
YALES2	256^3	384	1484	2.5	1.685	923	133	79
DINO	256^3	1024	13417	2.5	0.186	2414	39	210
Nek5000	253^3	576	3627	2.5	0.689	486	31	45
ProLB	256^3	256	160000	2.5	0.0156	2181	3	187
YALES2	256^3	768	1484	2.5	1.685	4109	594	354
DINO	256^3	1024	43628	2.5	0.057	5594	38	660
Nek5000	253^3	576	3527	2.5	0.709	4297	201	382 ^a
ProLB	256^3	256	160000	2.5	0.0156	2639	3.5	226

^a The publication²⁸ reports 283, but a quick calculation from the other columns indicates a typo.

TABLE I. The code performance comparison for the cold (top) and hot (bottom) cases. Units are as follows: $T_{\text{sim}}(\text{ms}_{\text{sim}})$; $\overline{\Delta t}(\mu\text{s}_{\text{sim}}/\text{iter})$; TCPU (hours); RCT ($\mu\text{s}_{\text{CPU}}/\text{iter.point}$); RTTS ($\mu\text{s}_{\text{CPU}}/\mu\text{s}_{\text{sim}}\text{iter.point}$).

Supplementary material is available, presenting the results from Steps 1 & 2 of the benchmark²⁸.

Part of this research was supported by ANR through MALBEC project (ANR-20-CE05-0009). Centre de Calcul Intensif d’Aix-Marseille is acknowledged for granting access to its high performance computing resources.

The data that support the findings of this study are available from the corresponding author upon reasonable request.

¹S. Chen and G. D. Doolen, “Lattice boltzmann method for fluid flows,” Annual review of fluid mechanics **30**, 329–364 (1998).

²T. Krüger, H. Kusumaatmaja, A. Kuzmin, O. Shardt, G. Silva, and E. M. Vigen, *The Lattice Boltzmann Method: Principles and Practice* (Springer, 2016).

³A. D’Hooge, L. Rebbeck, R. Palin, Q. Murphy, J. Gargoloff, and B. Duncan, “Application of real-world wind conditions for assessing aerodynamic drag for on-road range prediction,” Tech. Rep. (SAE Technical Paper, 2015).

⁴M. E. Gleason, B. Duncan, J. Walter, A. Guzman, and Y.-C. Cho, “Comparison of computational simulation of automotive spinning wheel flow field with full width moving belt wind tunnel results,” SAE International Journal of Passenger Cars-Mechanical Systems **8**, 275–293 (2015).

⁵M. R. Khorrami, E. Fares, B. Duda, and A. Hazir, “Compu-

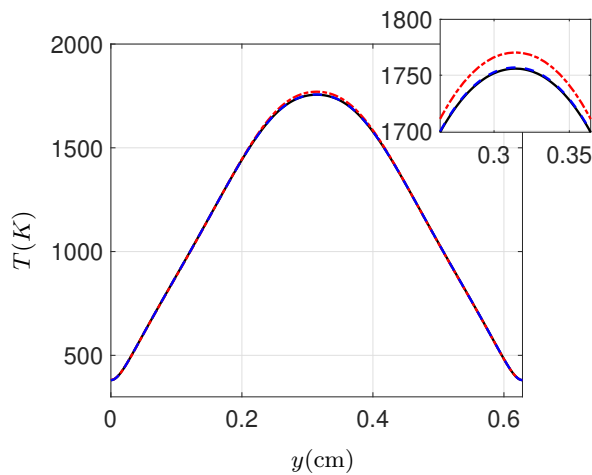


FIG. 3. Convergence study: Temperature plot from Fig. 2 repeated for 128^3 (dot-dashed), 256^3 (dashed) and 384^3 (solid) grids.

- tational evaluation of airframe noise reduction concepts at full scale,” in *22nd AIAA/CEAS Aeroacoustics Conference* (2016) p. 2711.
- ⁶M. R. Khorrami and E. Fares, “Simulation-based airframe noise prediction of a full-scale, full aircraft,” in *22nd AIAA/CEAS aeroacoustics conference* (2016) p. 2706.
- ⁷D. Casalino, A. Hazir, and A. Mann, “Turbofan broadband noise prediction using the lattice boltzmann method,” *AIAA Journal*, 1–20 (2017).
- ⁸G. Romani and D. Casalino, “Rotorcraft blade-vortex interaction noise prediction using the lattice-boltzmann method,” *Aerospace Science and Technology* (2019).
- ⁹R. Löhner, “Towards overcoming the LES crisis,” *International Journal of Computational Fluid Dynamics*, 1–11 (2019).
- ¹⁰O. Filippova and D. Hänel, “A Novel Lattice BGK Approach for Low Mach Number Combustion,” *Journal of Computational Physics* **158**, 139–160 (2000).
- ¹¹K. Yamamoto and N. Takada, “LB simulation on soot combustion in porous media,” *Physica A: Statistical Mechanics and its Applications* **362**, 111–117 (2006).
- ¹²E. Chiavazzo, I. V. Karlin, A. N. Gorban, and K. Boulouchos, “Coupling of the model reduction technique with the lattice Boltzmann method for combustion simulations,” *Combustion and Flame* **157**, 1833–1849 (2010).
- ¹³A. Xu, C. Lin, G. Zhang, and Y. Li, “Multiple-relaxation-time lattice boltzmann kinetic model for combustion,” *Physical Review E* **91**, 043306 (2015).
- ¹⁴K. Sun, S. Yang, and C. K. Law, “A diffuse interface method for simulating the dynamics of premixed flames,” *Combustion and Flame* **163**, 508–516 (2016).
- ¹⁵M. Ashna, M. H. Rahimian, and A. Fakhari, “Extended lattice boltzmann scheme for droplet combustion,” *Physical Review E* **95**, 053301 (2017).
- ¹⁶S. Hosseini, N. Darabiha, and D. Thévenin, “Mass-conserving advection–diffusion lattice boltzmann model for multi-species reacting flows,” *Physica A: Statistical Mechanics and its Applications* **499**, 40–57 (2018).
- ¹⁷C. Lin and K. H. Luo, “Mesoscopic simulation of nonequilibrium detonation with discrete boltzmann method,” *Combustion and Flame* **198**, 356–362 (2018).
- ¹⁸S. Hosseini, A. Abdelsamie, N. Darabiha, and D. Thévenin, “Low-mach hybrid lattice boltzmann-finite difference solver for combustion in complex flows,” *Physics of Fluids* **32**, 077105 (2020).
- ¹⁹S. A. Hosseini, A. Eshghinejadfard, N. Darabiha, and

- D. Thévenin, “Weakly compressible lattice boltzmann simulations of reacting flows with detailed thermo-chemical models,” *Computers & Mathematics with Applications* **79**, 141–158 (2020).
- ²⁰C. Lin and K. Luo, “Kinetic simulation of unsteady detonation with thermodynamic nonequilibrium effects,” *Combustion, Explosion, and Shock Waves* **56**, 435–443 (2020).
- ²¹Y. Feng, P. Boivin, J. Jacob, and P. Sagaut, “Hybrid recursive regularized thermal lattice boltzmann model for high subsonic compressible flows,” *Journal of Computational Physics* **394**, 82–99 (2019).
- ²²G. Farag, S. Zhao, T. Coratger, P. Boivin, G. Chiavassa, and P. Sagaut, “A pressure-based regularized lattice-boltzmann method for the simulation of compressible flows,” *Physics of Fluids* **32**, 066106 (2020).
- ²³M. Tayyab, S. Zhao, Y. Feng, and P. Boivin, “Hybrid regularized lattice-boltzmann modelling of premixed and non-premixed combustion processes,” *Combustion and Flame* **211**, 173–184 (2020).
- ²⁴M. Tayyab, B. Radisson, C. Almarcha, B. Denet, and P. Boivin, “Experimental and numerical lattice-boltzmann investigation of the darrieus-landau instability,” *Combustion and Flame* **221**, 103–109 (2020).
- ²⁵M. Tayyab, S. Zhao, and P. Boivin, “Lattice-boltzmann modelling of a turbulent bluff-body stabilized flame,” *Physics of Fluids* **33**, 031701 (2021).
- ²⁶X. He, S. Chen, and R. Zhang, “A lattice boltzmann scheme for incompressible multiphase flow and its application in simulation of rayleigh–taylor instability,” *Journal of Computational Physics* **152**, 642–663 (1999).
- ²⁷S. Zhao, G. Farag, P. Boivin, and P. Sagaut, “Toward fully conservative hybrid lattice boltzmann methods for compressible flows,” *Physics of Fluids* **32**, 126118 (2020).
- ²⁸A. Abdelsamie, G. Lartigue, C. E. Frouzakis, and D. Thévenin, “The taylor-green vortex as a benchmark for high-fidelity combustion simulations using low-mach solvers,” *Computers & Fluids* **223**, 104935 (2021).
- ²⁹A. Sengissen, J.-C. Giret, C. Coreixas, and J.-F. Bousuge, “Simulations of lagoon landing-gear noise using lattice boltzmann solver,” in *21st AIAA/CEAS Aeroacoustics Conference* (2015) p. 2993.
- ³⁰H. Touil, D. Ricot, and E. Lévêque, “Direct and large-eddy simulation of turbulent flows on composite multi-resolution grids by the lattice boltzmann method,” *Journal of Computational Physics* **256**, 220–233 (2014).
- ³¹G. Farag, S. Zhao, G. Chiavassa, and P. Boivin, “Consistency study of lattice-boltzmann schemes macroscopic limit,” *Physics of Fluids* **33**, 031701 (2021).
- ³²T. Poinso and D. Veynante, *Theoretical and numerical combustion* (RT Edwards, Inc., 2005).
- ³³S. Marié, D. Ricot, and P. Sagaut, “Comparison between lattice boltzmann method and navier–stokes high order schemes for computational aeroacoustics,” *Journal of Computational Physics* **228**, 1056–1070 (2009).
- ³⁴P. Saxena and F. Williams, “Testing a small detailed chemical-kinetic mechanism for the combustion of hydrogen and carbon monoxide,” *Combustion and Flame* **145**, 316–323 (2006).
- ³⁵P. Boivin, C. Jiménez, A. L. Sánchez, and F. A. Williams, “An explicit reduced mechanism for H₂–air combustion,” *Proceedings of the Combustion Institute* **33**, 517–523 (2011).
- ³⁶P. Boivin, A. Dauplain, C. Jiménez, and B. Cuenot, “Simulation of a supersonic hydrogen–air autoignition-stabilized flame using reduced chemistry,” *Combustion and Flame* **159**, 1779–1790 (2012).
- ³⁷P. Boivin, *Reduced-kinetic mechanisms for hydrogen and syngas combustion including autoignition*, Phd, Universidad Carlos III de Madrid (2011).
- ³⁸Y. Feng, M. Tayyab, and P. Boivin, “A lattice-boltzmann model for low-mach reactive flows,” *Combustion and Flame* **196**, 249–254 (2018).